IOWA STATE UNIVERSITY

UNIVERSITY OF MINNESOTA
Driven to Discover℠

KIT
Karlsruhe Institute of Technology

Enhanced nematic fluctuations near the Mott insulating phase of high-T_c cuprates

Peter P. Orth (Iowa State University)

In collaboration with B. Jeevanesan (Karlsruhe Institute of Technology, KIT), J. Schmalian (KIT) and R. M. Fernandes (University of Minnesota)

"Intertwined Order and Fluctuations in Quantum Materials" , KITP, 5 Sept 2017

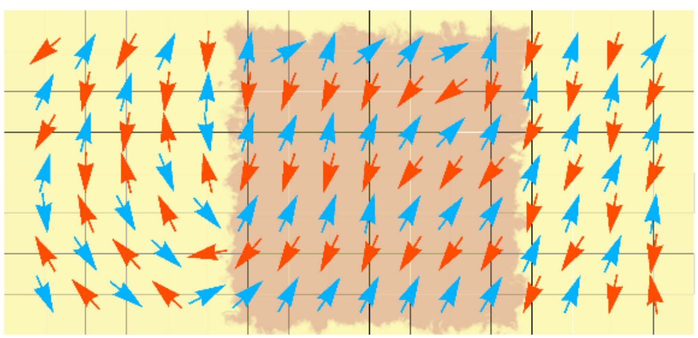

PPO, B. Jeevanesan, R. M. Fernandes, J. Schmalian, arXiv:1703:02210 (2017).

B. Jeevansan

J. Schmalian

R. M. Fernandes

Generic features of cuprate phase diagram

- Various features/phases are present among different families
- Much progress at experimental front
  - Neel AF (Mott/charge transfer insulator zero doping x=0)
  - Incommensurate SDW (small x) [1]
  - (fluctuating) charge order (NMR [2], RXS [3], X-Ray [4])
  - Pseudogap in quasi-particle spectrum [5]
  - Nematicity (resistivity anistropy [6], Nernst [7], STM [8], neutron scattering [1], torque magnetometry [9])
  - Superconductivity (at sufficiently large x)

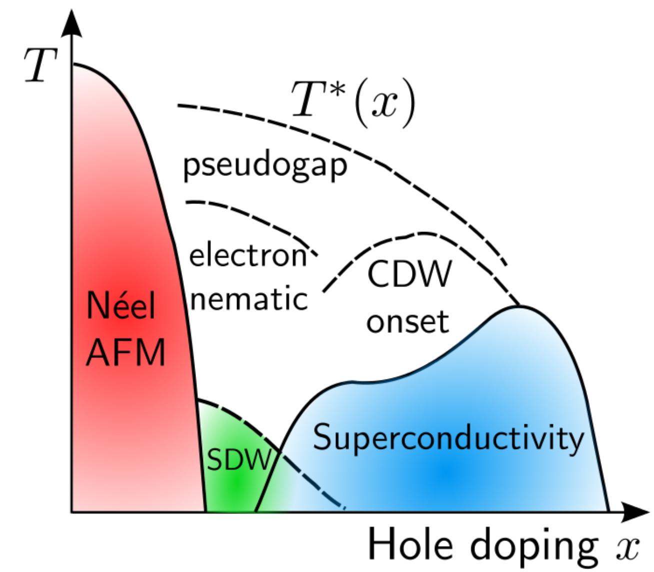

[1] D. Haug *et al.*, NJP **12**, 205006 (2010); [2] W. Wu et al., Nature **477**, 191 (2011); [3] G. Ghiringhelli et al., Science **337**, 821 (2012); [4] J. Chang et al., Nat. Phys. **8**, 871 (2012); [5] T. Kondo et al., Nature **457**, 296 (2009); [6] Y. Ando et al., PRL **88**, 137005 (2002); [7] R. Daou et al., Nature **463**, 519 (2010); [8] Y. Kohsaka et al., Science (2007); [9] Y. Sato et al., Nat. Phys. (2017).

Guiding principles in cuprate phase diagram

- Two guiding principles:
  - Novel phases other than SC only appear below $T^{*}(p)$
  - $T^{*}(p)$ increases monotonically as $p \to 0$ reaching $T^{*}(p) \to T_N$
  - Importance of short-range AF order
  - Here, we want to focus on electronic nematicity (in YBCO)

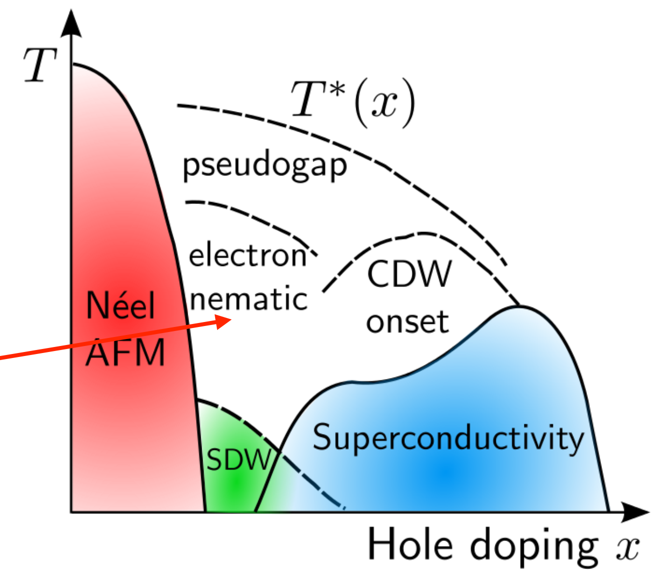

Connection of nematicity and short-range AF correlations?

[1] D. Haug *et al.*, NJP **12**, 205006 (2010); [2] W. Wu et al., Nature **477**, 191 (2011); [3] G. Ghiringhelli et al., Science **337**, 821 (2012); [4] J. Chang et al., Nat. Phys. **8**, 871 (2012); [5] T. Kondo et al., Nature **457**, 296 (2009); [6] Y. Ando et al., PRL **88**, 137005 (2002); [7] R. Daou et al., Nature **463**, 519 (2010); [8] Y. Kohsaka et al., Science (2007); [9] Y. Sato et al., Nat. Phys. (2017).

Experimental signatures of (spin) nematicity

Experimental signatures of nematicity in $YBa_2Cu_3O_{7-\delta}$

- Nematic order = electronic state breaking C_4 symmetry of CuO_2 plane
- $YBa_2Cu_3O_{7-\delta}$ has orthorhombic crystal structure for $\delta \leq 0.7$: $a \neq b$; $\delta = 0.7, 0.65, 0.55$ ($p \geq 0.05$)
- Inelastic neutron scattering peak close to Neel ordering wavevector $Q = (\pi, \pi)$ is elliptic [1]

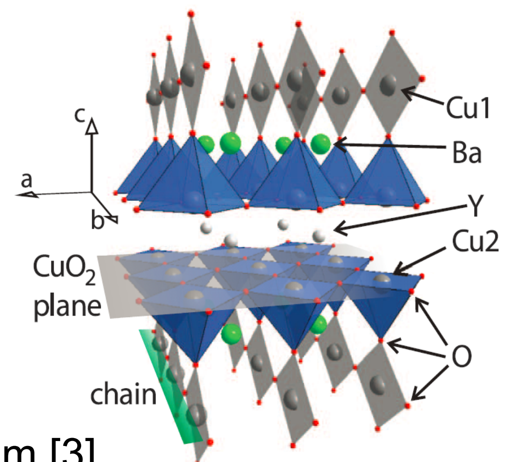

From [3]

$p = 0.05$, $T = 3K$

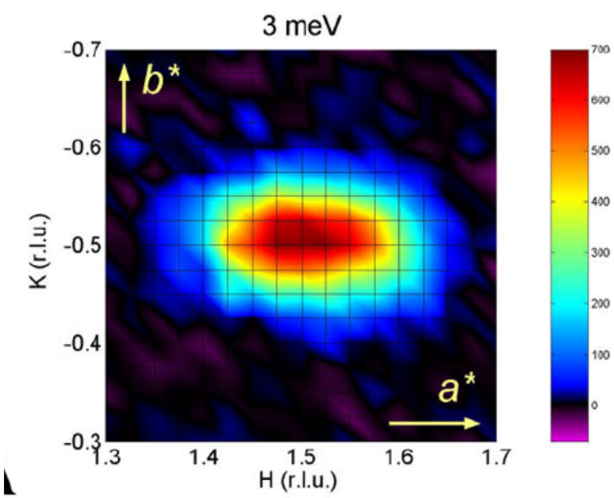

Location in PD:
Hole underdoped

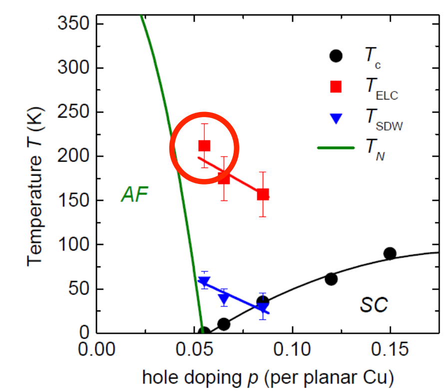

[1] D. Haug *et al.*, New J. Phys. **12**, 105006 (2010); [2] S. Kivelson et al. Nature 1998; [3] G. Ghiringhelli et al., Science **337**, 821 (2012); W. Metzner et al. PRL 2003, S. Sachdev et al. PRL 2013, Nie et al. PNAS 2014, Wang et al. PRB 2014, Fang et al. PRB 2008, Sun et al. PRL 2010, Kivelson et al. PRB 2004, Fischer et al. PRB 2011

Inelastic neutron scattering at low temperatures T=3K

- At lowest $T=3K$: (Quasi-)elastic peak close to $Q=(\pi, \pi)$ describing static incommensurate spin-density wave (SDW) order
- Inelastic contribution peaked at energy of 3 meV remains present at larger temperatures T

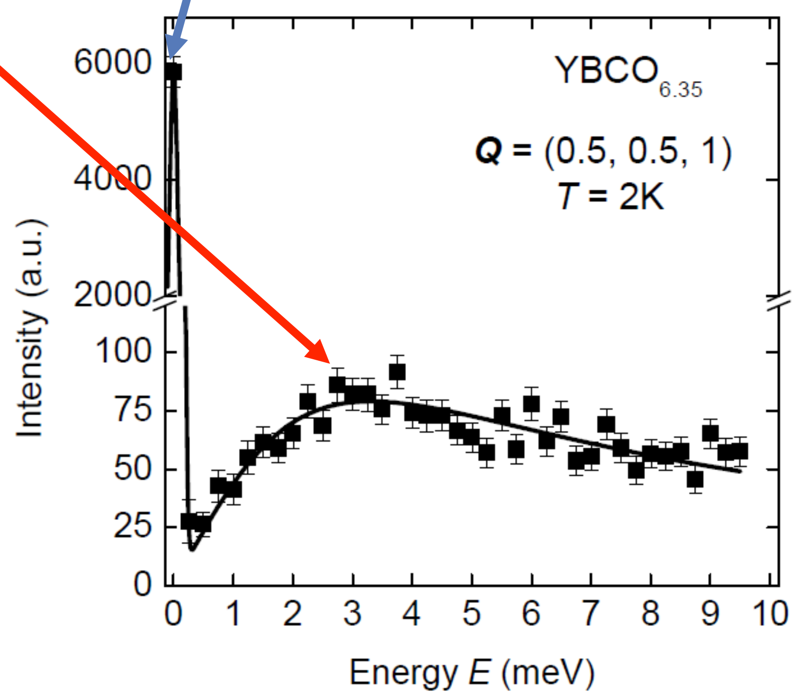

From [1]

[1] D. Haug *et al.*, New J. Phys. **12**, 105006 (2010).

Experimental signatures of nematicity in $YBa_2Cu_3O_{7-\delta}$

- Scattering peaks at $Q=(\pi,\pi)$ and energy $E \leq 7\ meV$ show in-plane anisotropy ($a \neq b$)
- Elliptical shape with major axis along a direction

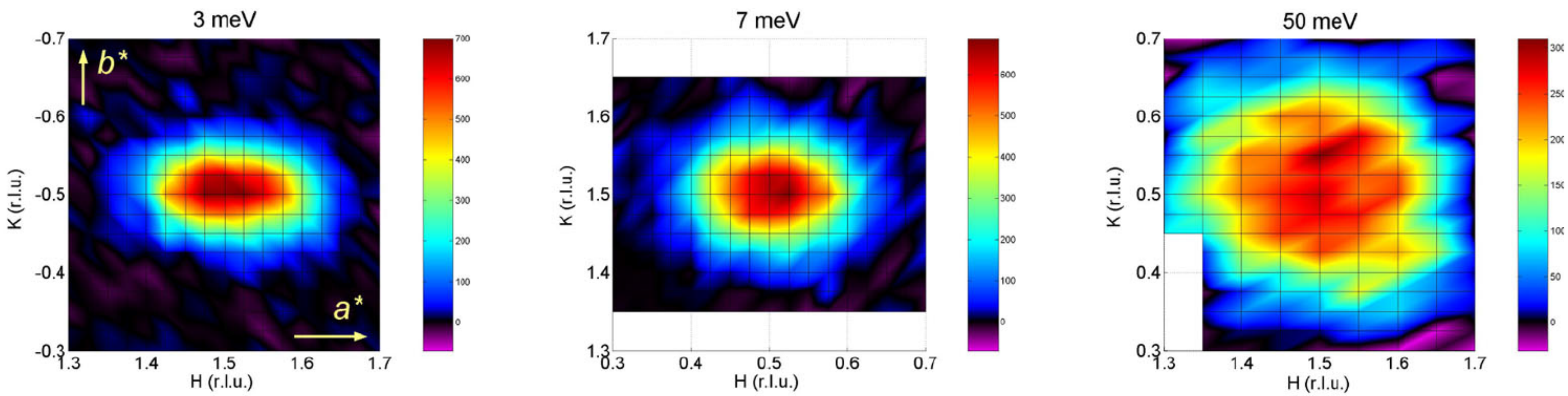

Increasing energy E

From [1]

$$\Delta_a > \Delta_b$$

Lowest doping $p=0.05$

[1] D. Haug *et al.*, New J. Phys. **12**, 105006 (2010).

Experimental signatures of nematicity in $YBa_2Cu_3O_{7-\delta}$

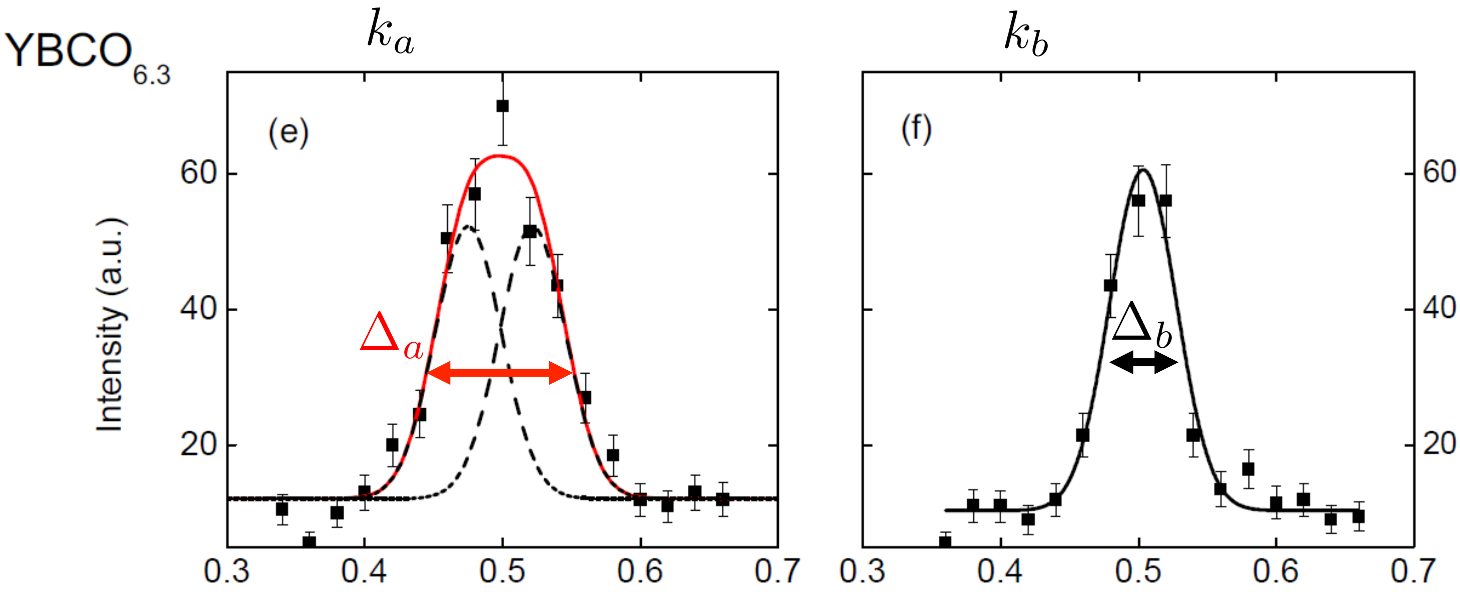

From [1]

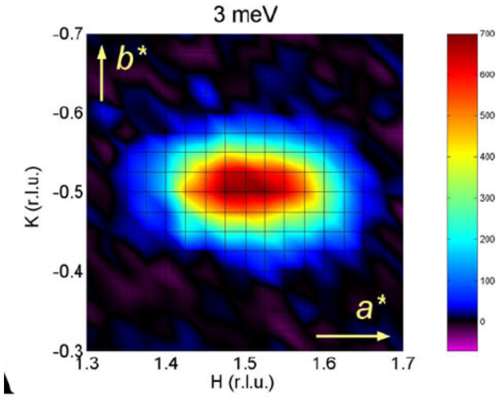

Lowest doping p=0.05

$\Delta_a > \Delta_b$

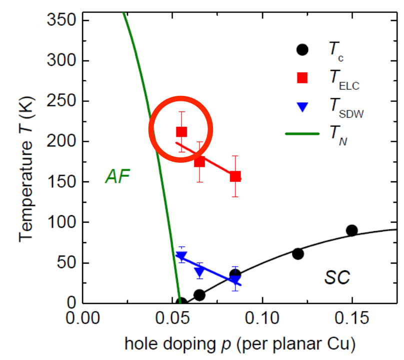

T=3K, E=3meV, k=1.55/A

[1] D. Haug *et al.*, New J. Phys. **12**, 105006 (2010).

Experimental signatures of nematicity in $YBa_2Cu_3O_{7-\delta}$

- Ellipticity $(\Delta_a - \Delta_b)$ increases with hole doping p

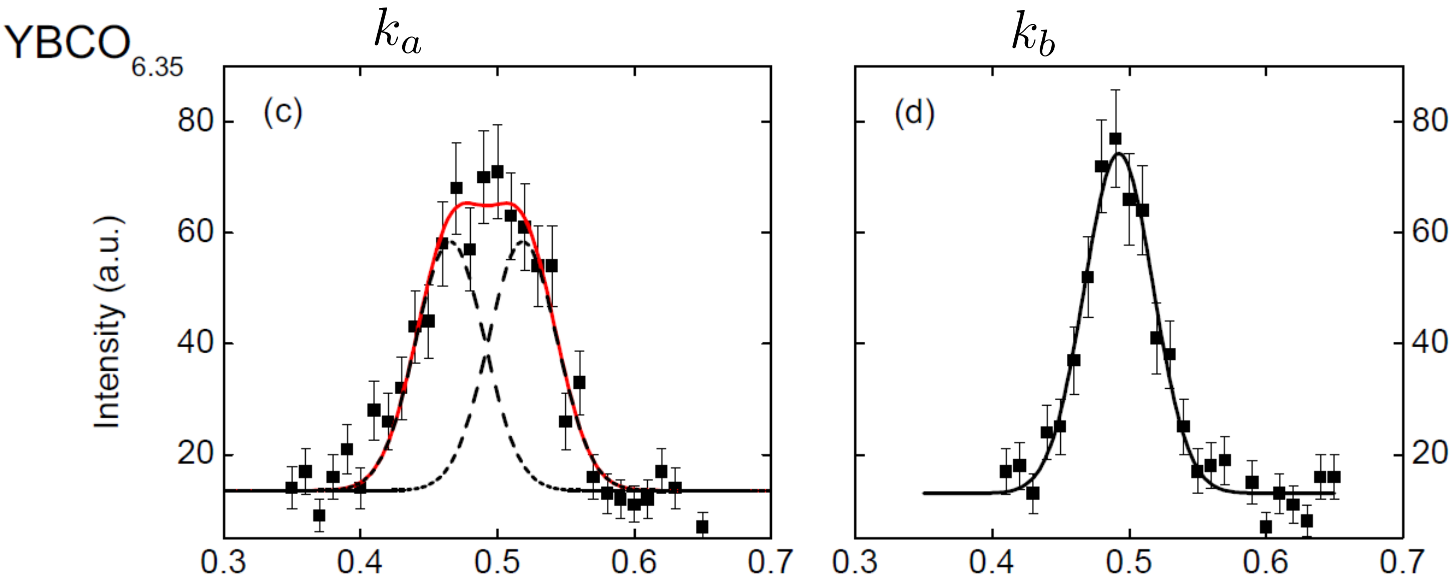

From [1]

Larger doping p=0.06

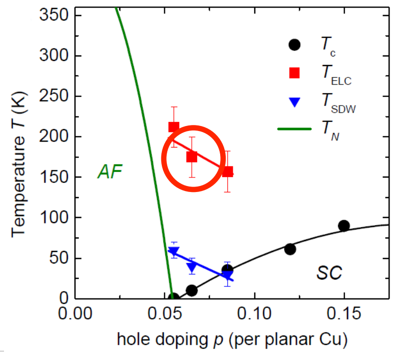

[1] D. Haug *et al.*, New J. Phys. **12**, 105006 (2010).

Experimental signatures of nematicity in $YBa_2Cu_3O_{7-\delta}$

- Scattering peaks eventually split: incommensurate wavevectors along a

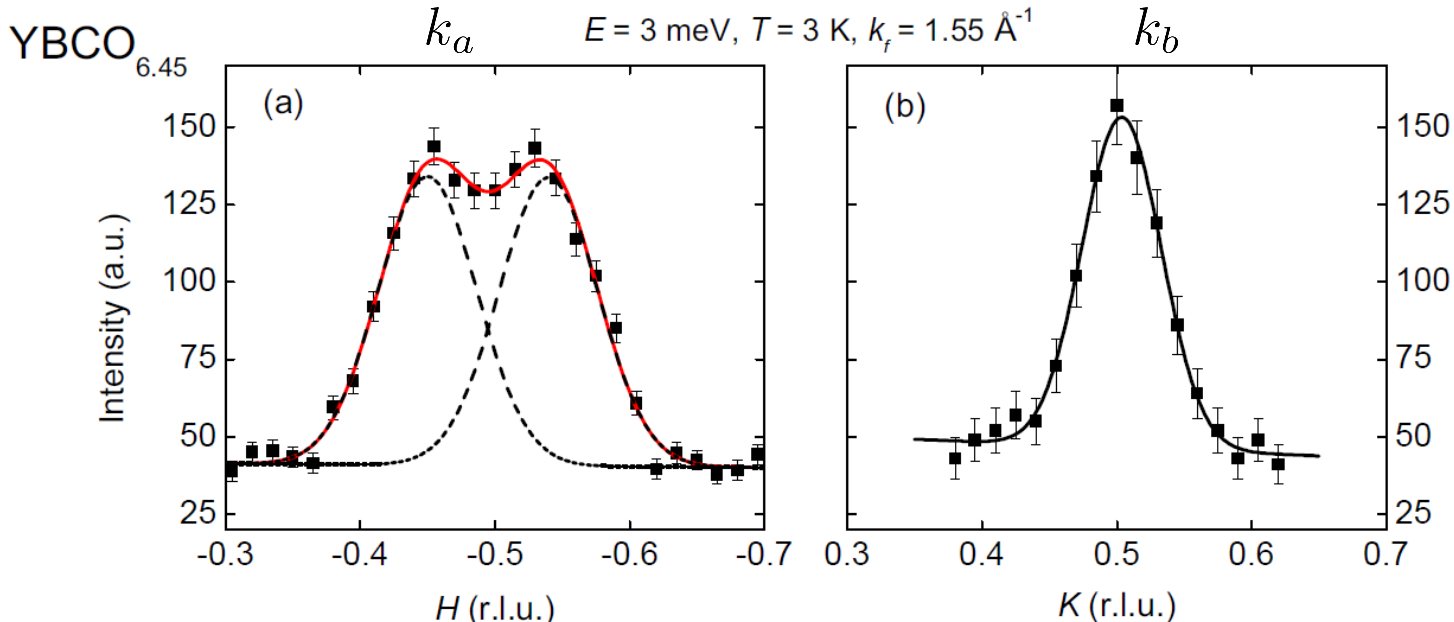

From [1]

Largest doping p=0.08

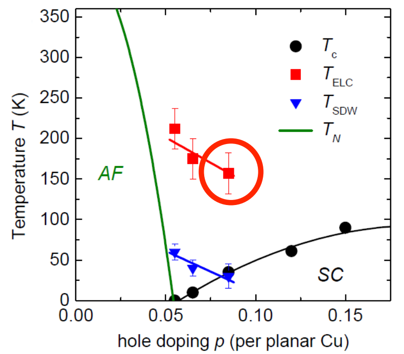

[1] D. Haug *et al.*, New J. Phys. **12**, 105006 (2010).

Summary of nematicity signatures in inelastic neutron

- Small ellipticity present even above T_{nem} due to orthorhombic distortion of YBCO
- T-dependent ellipticity of inealistic peaks appears at large $T_{nem} \approx 150\ K$
- Ellipticity increases with lowering T
- Doping-dependent onset temperature $T_{nem}(p)$
- Incommensurate SDW onsets at same doping

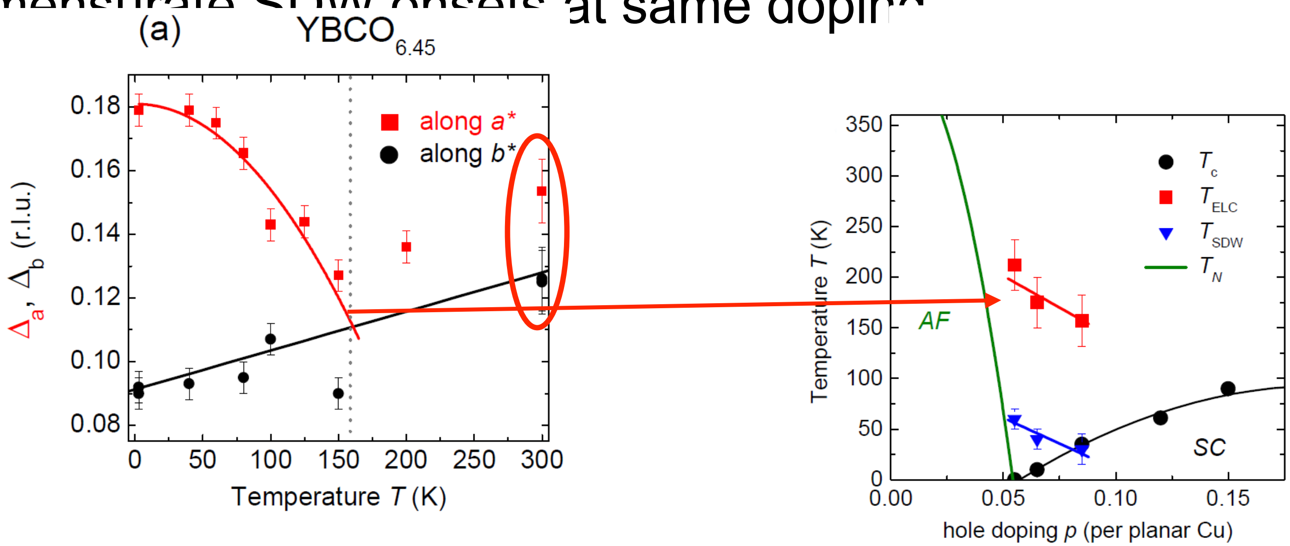

From [1]

[1] D. Haug *et al.*, New J. Phys. **12**, 105006 (2010). [2] J. Chang et al., Nat. Phys. **8**, 871 (2012). [3] M. Vojta, Adv. Phys. **58**, 699 (2009); [4] L. Nie *et al.*, arXiv:1701:02751 (2017).

Summary of nematicity signatures in inelastic neutron

- Small ellipticity present even above T_{nem} due to orthorhombic distortion of YBCO
- T-dependent ellipticity of inealistic peaks appears at large $T_{nem} \approx 150\ K$
- Ellipticity increases with lowering T
- Doping-dependent onset temperature $T_{nem}(p)$
- Incommensurate SDW onsets at same doping

From [2]

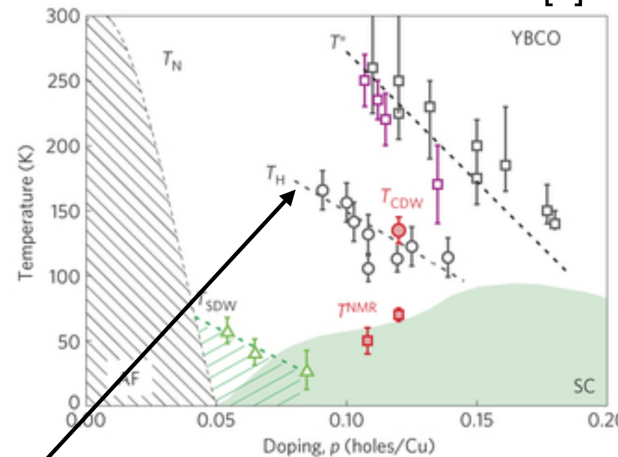

Other signatures of nematic “stripe” correlations

- Appears only for hole doping
- Appears only when tetragonal symmetry is explicitly broken (new data by Matsuda *et al.*?)
- (Fluctuating) stripe CDW nearby
- Appears at “large” temperatures scales $T \sim J$

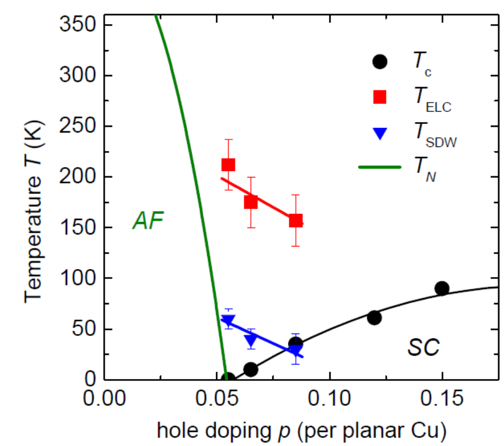

From [1]

[1] D. Haug *et al.*, New J. Phys. **12**, 105006 (2010). [2] J. Chang et al., Nat. Phys. **8**, 871 (2012). [3] M. Vojta, Adv. Phys. **58**, 699 (2009); [4] L. Nie *et al.*, arXiv:1701:02751 (2017).

Summary of nematicity signatures in inelast. neutron

- T-dependent ellipticity of inealistic peaks appears at large $T\downarrow nem \approx 150\ K$
- Doping-dependent onset temperature $T\downarrow nem$ (p)
- Ellipticity increases with lowering T
- Incommensurate SDW onsets at same doping
- Small ellipticity present even above $T\downarrow nem$ due to orthorhombic distortion of YBCO

From [2]

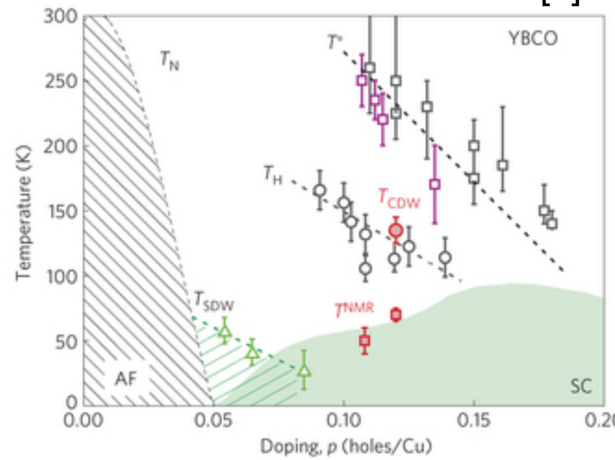

We now describe microscopic mechanism by which nematicity appears close to AF Neel order.

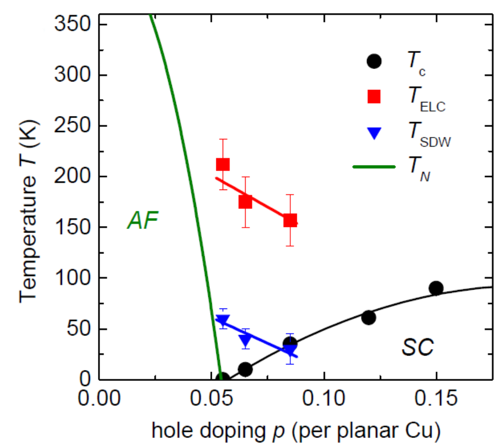

Theory program:

- Microscopic derivation of biquadratic spin exchange K term from 3-band Hubbard model
- Analysis of biquadratic K term including classical and quantum fluctuations

Microscopic derivation of biquadratic spin exchange

Microscopic starting point: 3-orbital Hubbard model

- Three-band Hubbard model: Cu $d_{x^2-y^2}$, O p_x, p_y orbitals

$$H = H_\epsilon + H_t + H_U + H_V$$

Non-interacting part $H_t + H_\epsilon$

- hopping $t_{pd} > t_{pp}$
- orbital energy difference $\Delta = \epsilon_p - \epsilon_d > 0$.

On-site interactions

$$H_U = \sum_{\boldsymbol{R}_i} \left[U_{dd} n^d_{i\uparrow} n^d_{i\downarrow} + \frac{U_{pp}}{2} \left(n^p_{xi\uparrow} n^p_{xi\downarrow} + n^p_{yi\uparrow} n^p_{yi\downarrow} \right) \right]$$

Nearest-neighbor interactions

$$H_V = V_{pp} \sum_{\boldsymbol{R}_i,\sigma,\sigma'} \sum_{\delta'} n^p_{xi} n^p_{yi+\delta'} + V_{pd} \sum_{\delta} n^d_{xi} n^p_{i+\delta}$$

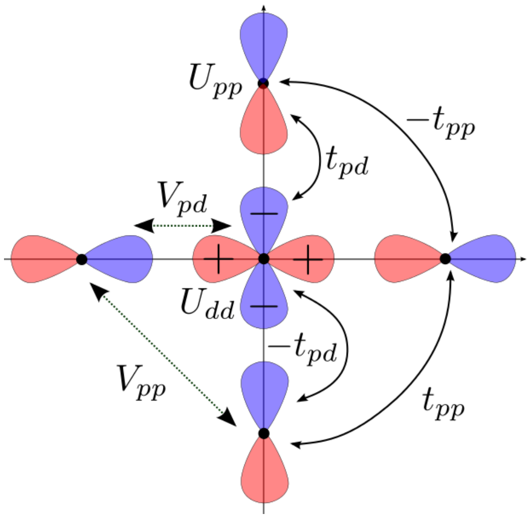

Undoped "vacuum state": One hole per Cu, filled O orbitals

➡ Charge-transfer (Mott) insulator: $t_{ij} \ll U_{dd}, \Delta$

➡ Strong-coupling expansion in $t_{ij}/U_{dd} - \Delta, t_{ij}/\Delta$ yields $t-J$-model describing mobile holes coupled to localized Cu spins. Role of oxygen density fluctuations?

Relevant terms in strong-coupling expansion

- Focus on subspace of singly occupied Cu spins first
- At second order
  - effective hole hopping between oxygens renormalizing $t{\downarrow}pp$
  - Cu-O Kondo-like exchange coupling $\propto \boldsymbol{S}_i \cdot \boldsymbol{s}_{jk}$

Cu spins: $$\boldsymbol{S}_j = \frac{1}{2}\sum_{\alpha,\beta} \tilde{d}^\dagger_{j\alpha} \boldsymbol{\sigma}_{\alpha\beta} \tilde{d}_{j\beta}$$

$$\tilde{d}_{j\alpha} = (1 - n_{j\bar{\alpha}} d^\dagger_{j\alpha}$$

(Non-)local oxygen spins: $$\boldsymbol{s}_{jk} = \frac{1}{2}\sum_{\alpha,\beta} p^\dagger_{j\alpha} \boldsymbol{\sigma}_{\alpha\beta} p_{k\beta}$$

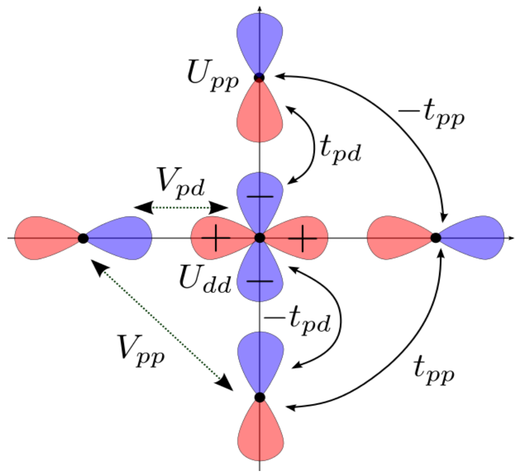

[1] E. Kolley *et al.*, J. Phys C **4**, 3517 (1992).

Relevant terms in Cu spin model

- At second order
  - effective hole hopping between oxygens renormalizing $t{\downarrow}pp$
  - Cu-O Kondo-like exchange coupling $\propto \boldsymbol{S}_i \cdot \boldsymbol{s}_{jk}$
- At fourth order
  - Heisenberg exchange of Cu spins
  - Non-local exchange of oxygen spins $H_J = J \sum_{\langle i,j \rangle} \boldsymbol{S}_i \cdot \boldsymbol{S}_j$
  - Cu-O Kondo-like exchange couplings
  - Oxygen density $n{\uparrow}p$ dependent Heisenberg exchange of Cu spins

$$H_{J'} = -J' \sum_{i,\delta} n^p_{i+\frac{\delta}{2}} \boldsymbol{S}_i \cdot \boldsymbol{S}_{i+\delta}$$

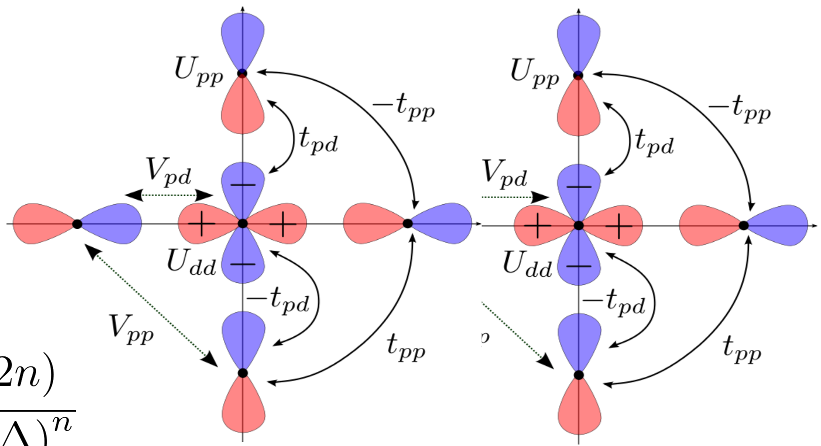

Exchange constants are of the same order:

$$J = \sum_{n=0}^{2} \frac{t_{pd}^4 (4 - n^2 - \delta_{n,2})}{2\Delta^{3-n}(U_{dd} - \Delta)^n} \qquad J' = \sum_{n=0}^{3} \frac{t_{pd}^4 \mathrm{sign}\,(3 - 2n)}{\Delta^{3-n}\,(U_{dd} - \Delta)^n}$$

[1] E. Kolley *et al.*, J. Phys C **4**, 3517 (1992).

Effect of oxygen charge flucutations

- Oxygen density $n↑p$ dependent Heisenberg exchange of Cu spins
  - Effect of quadrupolar oxygen charge fluctuations

$$H_{J'} = -J' \sum_{i,\delta} n^p_{i+\frac{\delta}{2}} \boldsymbol{S}_i \cdot \boldsymbol{S}_{i+\delta} = -J' \sum_i \left(n^p_{i+\frac{\hat{x}}{2}} \boldsymbol{S}_i \cdot \boldsymbol{S}_{i+\hat{x}} + n^p_{i+\frac{\hat{y}}{2}} \boldsymbol{S}_i \cdot \boldsymbol{S}_{i+\hat{y}} \right)$$

$$n^p_{i+\hat{x}} = (\bar{n}^p_i + \eta_i)/2$$

$$n^p_{i+\hat{y}} = (\bar{n}^p_i - \eta_i)/2$$

$$-J' \sum_i \frac{\eta_i}{2} \left(\boldsymbol{S}_i \cdot \boldsymbol{S}_{i+\hat{x}} - \boldsymbol{S}_i \cdot \boldsymbol{S}_{i+\hat{y}} \right)$$

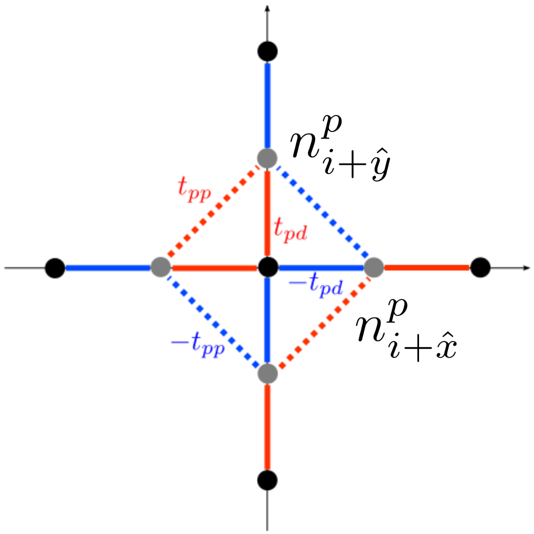

Biquadratic spin exchange term K

$$-J' \sum_i \frac{\eta_i}{2} \left(\boldsymbol{S}_i \cdot \boldsymbol{S}_{i+\hat{x}} - \boldsymbol{S}_i \cdot \boldsymbol{S}_{i+\hat{y}} \right)$$

Effect of quadrupolar oxygen charge fluctuations

- Decoupling oxygen interactions in the nematic channel η
- Integrating out oxygen degrees of freedom

$$H_K = -K \sum_i \left[\boldsymbol{S}_i \cdot \left(\boldsymbol{S}_{i+\hat{x}} - \boldsymbol{S}_{i+\hat{y}} \right) \right]^2 \quad \text{with} \quad K = \frac{J'^2}{2} \lim_{\mathbf{k}\to 0} \frac{\Pi^\eta_{\mathbf{k}}}{1 - U_{\mathbf{k}} \Pi^\eta_{\mathbf{k}}} > 0$$

$$U_{\mathbf{k}=\mathbf{0}} = V_{pp} - \frac{U_{pp}}{8}$$

Biquadratic spin exchange term, enhanced by O-O repulsion

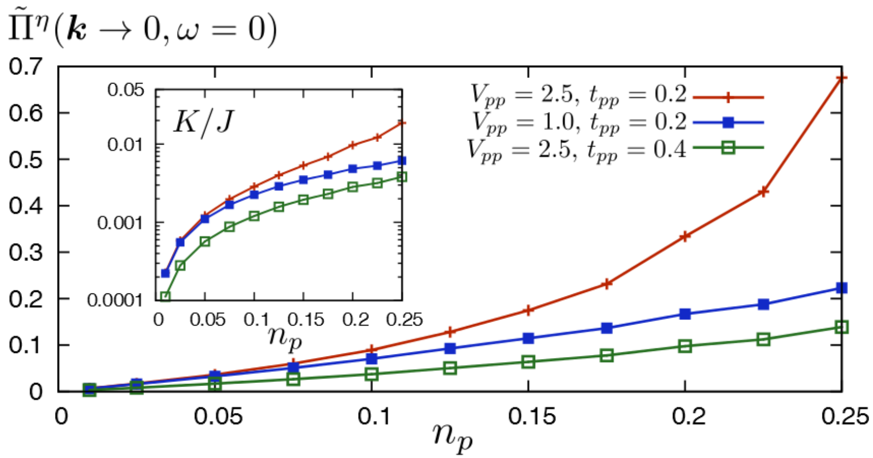

Π^η: Bare oxygen charge susceptibility in quadrupolar channel

- $\propto n_p$ at small doping
- Enhanced by large V_{pp} and small t_{pp}
- K/J up to a few percent

$$T = 10^{-2} t_{pp},\ n_d = 1,\ t_{pd} = 1,\ \Delta = 2.5,\ U_{dd} = 9,\ U_{pp} = 3,\ V_{pd} = V_{pp}$$

Analysis of t-J-K model at half-filling (first step)

Generalized t-J-K model

- Must include biquadratic exchange K term in t-J model

$$H_{t-J-K} = \sum_{ij\alpha} t_{ij} \tilde{d}^{\dagger}_{i\alpha} \tilde{d}_{j\alpha} + J \sum_{\langle ij \rangle} \left(\mathbf{S}_i \cdot \mathbf{S}_j - \frac{1}{4} n_i n_j \right)$$
$$- K \sum_i \left[\mathbf{S}_i \cdot \left(\mathbf{S}_{i-\hat{x}} + \mathbf{S}_{i+\hat{x}} - \mathbf{S}_{i-\hat{y}} - \mathbf{S}_{i+\hat{y}} \right) \right]^2$$

- Analyze K-term at half-filling of Cu sites
  - Does not modify spin-wave spectrum [1], because $H_K |\text{Néel}\rangle = 0$
  - Supports local "stripe" like fluctuations in Neel phase

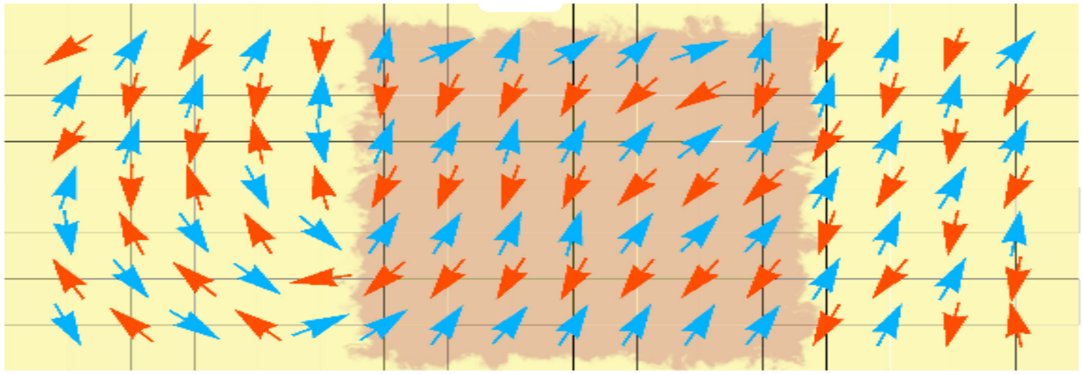

[1] R. Coldea *et al.*, PRL **86**, 5377 (2000).

Classical Monte-Carlo simulation of J-K model

- Composite "nematic" spin variable: $\varphi_i = \mathbf{S}_i \cdot (\mathbf{S}_{i-\hat{x}} + \mathbf{S}_{i+\hat{x}} - \mathbf{S}_{i-\hat{y}} - \mathbf{S}_{i+\hat{y}})$
- Static nematic response

$$\chi_{\text{nem}}(T) = \int_0^{1/T} d\tau \sum_i \langle \mathcal{T}_\tau \varphi_i(\tau) \varphi_0(0) \rangle$$

- Enhanced response in nematic $B\downarrow 1g$ channel
- Peaks at large $T \approx J$
- Enhancement $\propto K$
- Vanishes for $T \to 0$ as thermal fluctuations are suppressed. Disagrees with experimental observation.

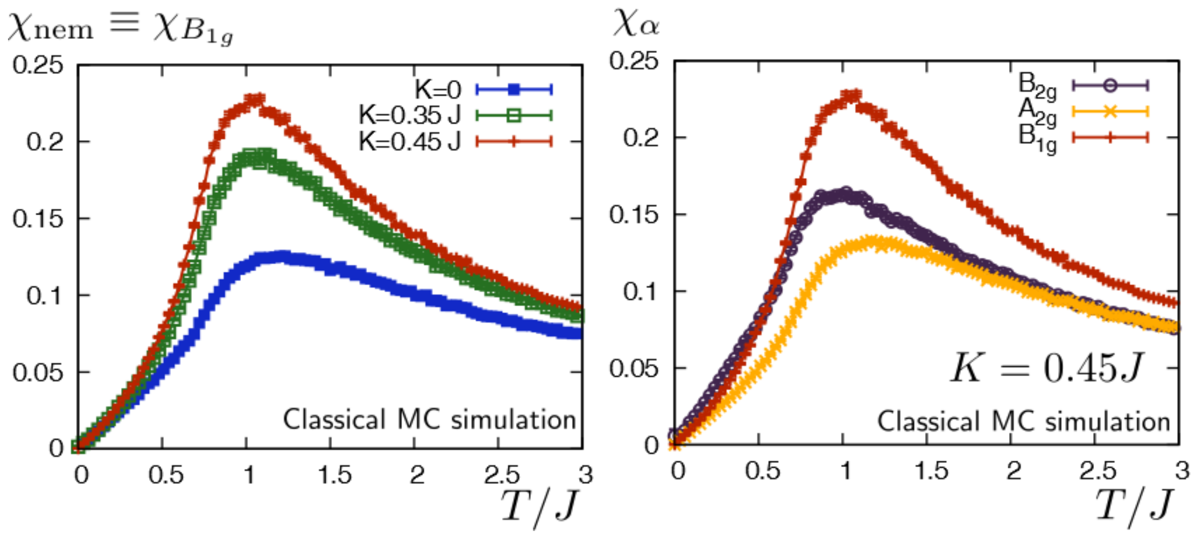

Quantum fluctuations within large-N approach

- Effective soft-spin action after decoupling in nematic channel

$$S = S_{\mathrm{dyn}} + \int_r \left[(\nabla \mathbf{n}_r)^2 - \varphi_r \left((\partial_x \mathbf{n}_r)^2 - (\partial_y \mathbf{n}_r)^2 \right) \right] + \int_r \left[r_0 \mathbf{n}_r^2 + \frac{u}{2} (\mathbf{n}_r \cdot \mathbf{n}_r)^2 + \frac{\varphi_r^2}{2g} - h_r \varphi_r \right]$$

Neel order parameter $\boldsymbol{n}_r$

$g \propto K/J$

Orthorhombic distortion field h_r

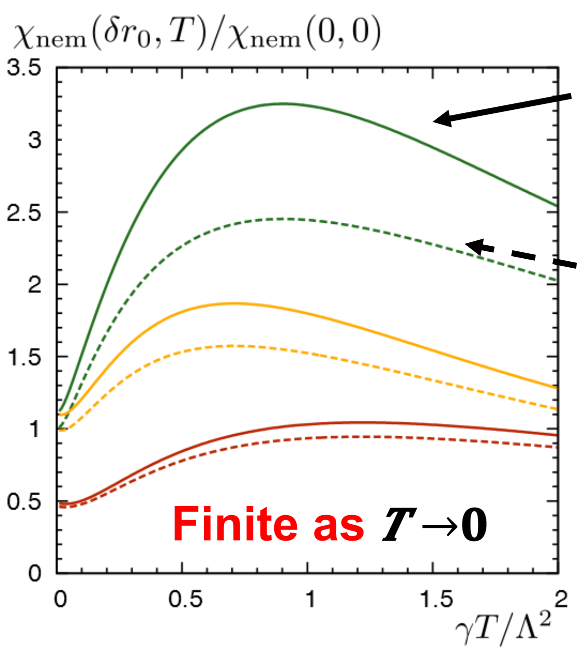

Full Susceptibility $\chi_{\mathrm{nem}} = \dfrac{\chi_{\mathrm{nem}}^{(0)}}{1 - \frac{g}{N}\chi_{\mathrm{nem}}^{(0)}}$

Bare susceptibility $\chi_{\mathrm{nem}}^{(0)} = \dfrac{N}{2} \displaystyle\int_q \dfrac{|\boldsymbol{q}|^4 \cos^2(2\theta)}{(\xi^{-2} + |\boldsymbol{q}|^2 + f(\omega_n))^2}$

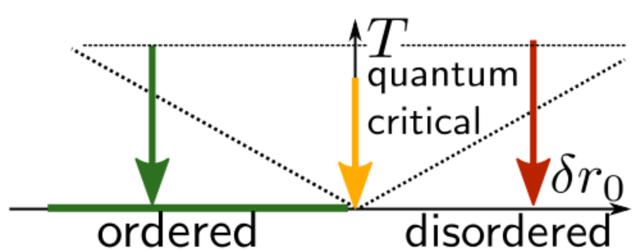

Changing temperature at fixed doping

Quantum fluctuations within large-N approach

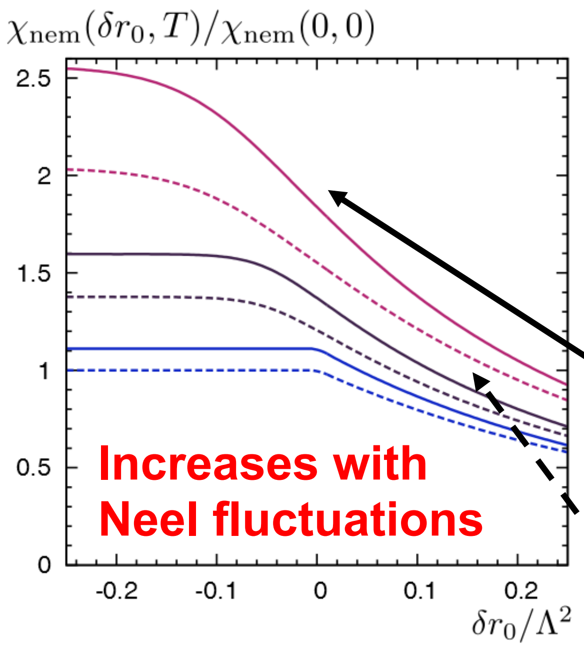

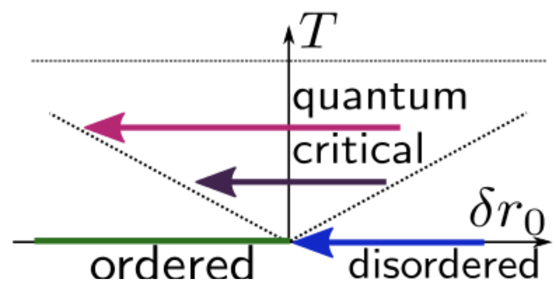

Changing doping or pressure at fixed T

Full Susceptibility $\chi_{\rm nem} = \dfrac{\chi^{(0)}_{\rm nem}}{1 - \frac{g}{N}\chi^{(0)}_{\rm nem}}$

Bare susceptibility $\chi^{(0)}_{\rm nem} = \dfrac{N}{2}\displaystyle\int_q \frac{|\boldsymbol{q}|^4 \cos^2(2\theta)}{\left(\xi^{-2} + |\boldsymbol{q}|^2 + f(\omega_n)\right)^2}$

- Nematic susceptibility is not universal at Neel quantum critical point (QCP)
- Depends on microscopic details such as a in $r_0 = a(T - T_c)$

Example: qualitative behavior above QCP depends on a

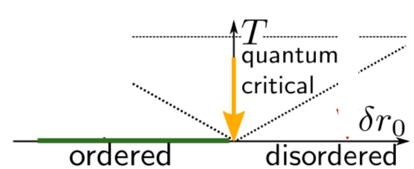

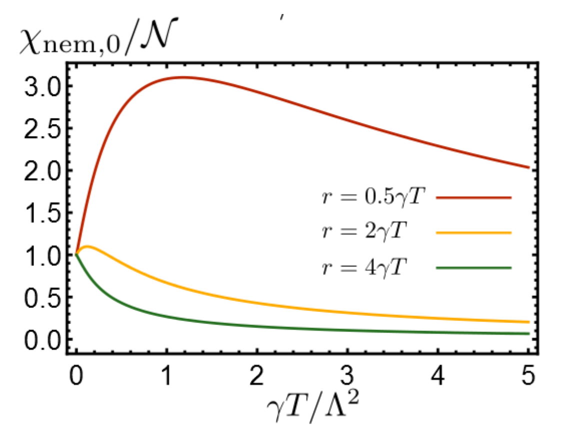

Finite nematic order in symmetry breaking field

- Nematic susceptibility large but not divergent
- Finite nematic order $\langle \varphi \rangle = \langle S_i (S_{i+x} - S_{i+y}) \rangle = \chi_{nem} h_r$ only in presence of symmetry-breaking field
- Symmetry-breaking field given by CuO chains in YBCO.
- Prediction: similar behavior in tetragonal system under applied strain

Finite φ leads to elliptic magnetic scattering peaks

$$\chi_{\mathrm{AFM}}\left(\mathbf{Q}+\mathbf{q},\omega\right) = \frac{1}{\xi^{-2} + \mathbf{q}^2 - \varphi\left(q_x^2 - q_y^2\right) + f\left(\omega_n\right)}$$

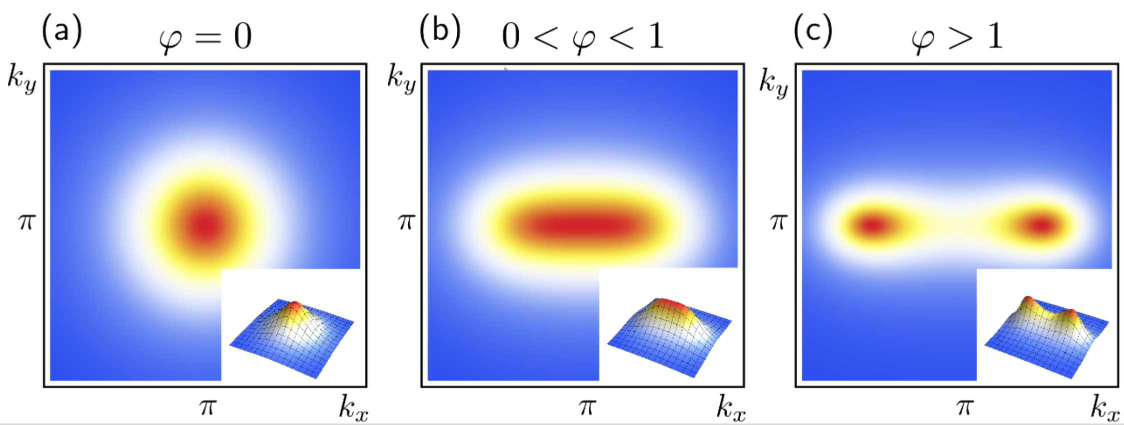

Incommensurability transition induced by nematic order. Explains common onset [1].

Alternative scenario: nematic order vestige to SDW [2]

[1] D. Haug *et al.*, NJP **12**, 205006 (2010); [2] L. Nie *et al.*, arXiv:1701:02751 (2017).

Conclusion

Electronic nematicity in cuprates due to

- Short-range “stripe” AFM correlations due to biquadratic spin exchange K
- Large, but non diverging nematic susceptibility χ_{nem} and presence of a symmetry breaking field h_r (e.g. oxygen chains or external strain)
- Enhanced by large quadrupolar oxygen density fluctuations due to repulsive interactions V_{pp}.
- Include biquadratic exchange term in generalized $t-J-K$ model to describe lightly hole-doped cuprates

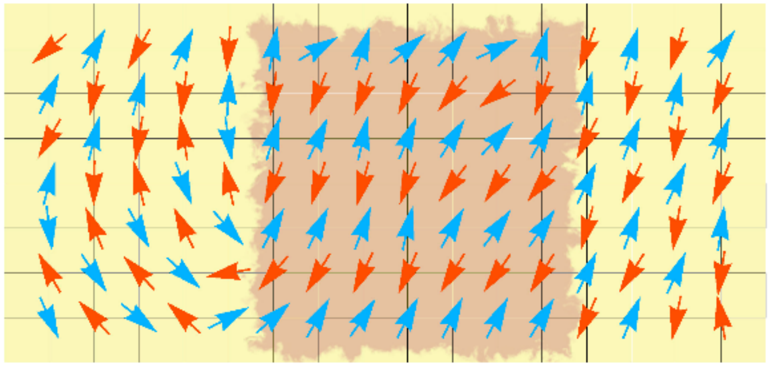

PPO, B. Jeevanesan, R. M. Fernandes, J. Schmalian, arXiv:1703:02210 (2017).

Explains:

- Ellipticity of neutron peaks
- Common onset of incommensurate SDW order
- Why nematicity is only observed on hole doped side
- Why only observed if tetragonal symmetry is explicitly broken

Thank you for your attention.